

# Structural Investigations of Si/C/N-Ceramics from Polysilazane Precursors by Nuclear Magnetic Resonance

Juliane Seitz,<sup>a</sup> Joachim Bill,<sup>a</sup> Norbert Egger<sup>b</sup> & Fritz Aldinger<sup>a</sup>

<sup>a</sup>Max-Planck-Institut für Metallforschung, Institut für Werkstoffwissenschaft, Pulvermetallurgisches Laboratorium, Heisenbergstrasse, D70569, Stuttgart, Germany

<sup>b</sup>Hoechst AG, Analytisches Laboratorium, Frankfurt, Germany

(Received 13 April 1995; accepted 18 November 1995)

## Abstract

*Polymeric precursors to Si/C/N-ceramics can be obtained by thermal crosslinking of polysilazanes. The precursor is then pyrolysed at a temperature of 1000°C into the amorphous ceramic. Between 1000 and 2000°C this amorphous state is transformed into the thermodynamically stable phases. The processes during pyrolysis and crystallization are connected with microstructural conversion. Simultaneously, changes of chemical and physical properties take place. The successive conversion of the atomic coordination during the transformation from the polymer into the amorphous ceramic and finally into the crystalline ceramic was studied using solid-state NMR. <sup>29</sup>Si-, <sup>13</sup>C- and <sup>1</sup>H-spectra were recorded. The result is a detailed report of the reactions and changes in structure occurring during ceramization of a polyhydromethylsilazane and crystallization of its ceramic residue. Furthermore, the amorphous state of this material was compared with a polyvinylsilazane-derived amorphous ceramic.*

## 1 Introduction

As already reported<sup>1–3</sup> thermal crosslinking of inorganic Si/C/N-polymers leads to the formation of infusible polymeric precursors with increased molecular weight. These precursors are pyrolysed into amorphous single-phase materials at 1000°C. Above 1000°C the thermodynamically stable phases silicon carbide and silicon nitride are formed. The resulting SiC/Si<sub>3</sub>N<sub>4</sub>-ceramics are free of sintering additives. These ceramics are therefore interesting materials for high temperature applications as they have a high thermal and chemical stability.

The changes in chemical structure during the transformation polymer–amorphous material–

crystalline ceramic are investigated by means of solid-state NMR. Knowing the reactions during the conversion allows control of the desired attributes of the resulting ceramic by specific variation of the polymer or the reaction conditions. The NMR experiments show the appropriate atomic coordination which gives information about the molecular structure of the samples.

In this report, the polyhydromethylsilazane NCP 200 (commercial product, Nichimen<sup>®</sup>, Japan) was studied. The copolymer consists of the structure  $[-SiHMe-NH-]_m[-SiMe_2-NH-]_n$  and has a molecular weight of 1100 g/mol. The reactions and intermediates occurring between RT and 1800°C are investigated in detail and the molecular structures for selected temperatures are determined. In addition, the amorphous state of a polyvinylsilazane, named VT 50 (Hoechst AG), was studied and compared with the single-phase material derived from the NCP 200 mentioned above. Polyvinylsilazane VT 50 contains  $[-SiVi(NH)_2-]$ -structural units and a small number of end groups  $[-SiVi(NH)-NMe_2-]$ . This polymer has a molecular weight of 800 g/mol.

## 2 Experimental

Below 1100°C the thermal treatment of the polysilazanes was carried out in quartz tubes in a slight argon flow. The heating rate was 25°C/h. The appropriate temperatures were held for 4 h. Further annealing of the pyrolysed samples at temperatures above 1100°C was carried out for 50 h (heating rate: 120°C/h) in a nitrogen atmosphere using a silicon nitride powder bed.

The NMR-experiments were performed on a Bruker MSL 300 at Hoechst AG, Frankfurt, Germany. The resonance frequency for <sup>1</sup>H was 300.13 MHz, for <sup>13</sup>C 75.47 MHz and for <sup>29</sup>Si

59.60 MHz. All spectra were acquired using magic angle spinning (MAS) with a rotation frequency of 4500 Hz. The excitation of the observed nucleus was 3  $\mu$ s for  $^1\text{H}$ , 4  $\mu$ s for  $^{13}\text{C}$  and 5  $\mu$ s for  $^{29}\text{Si}$  when the single pulse technique was used. This technique was applied for the measurement of all samples. All spectra were  $^1\text{H}$ -decoupled during the data acquisition. The samples heated above 1400°C needed long relaxation times, up to 10 min repetition time was required but time  $T_1$  was not measured explicitly. The number of scans varied and was optimized to get an acceptably good signal to noise ratio. The samples heated below 1100°C were also measured with a crosspolarization sequence (CP). The contact time for  $^{13}\text{C}$  and  $^{29}\text{Si}$  was 1 and 5 ms respectively. The repetition time was 10 s.

### 3 Results and Discussion

#### 3.1 NCP 200

##### 3.1.1 Polymer

The  $^{13}\text{C}$ -spectrum (Fig. 1) of the polymer shows a sharp peak at 5 ppm which is caused by the carbon of the silylmethyl group  $\text{Si}-\text{CH}_3$ .<sup>4</sup>

The  $^{29}\text{Si}$ -spectrum (Fig. 2) shows three sharp signals. The peak with the chemical shift of -22 ppm

is assigned to a  $\text{SiN}_2\text{CH}$  environment.<sup>5,6</sup> This is proven by the comparison of CP- and one-pulse-spectra. As expected, the  $\text{SiN}_2\text{CH}$  signal in the one-pulse-spectrum is weaker than in the CP-spectrum because a signal with a Si-H-bond is detected more strongly in the CP-spectrum. The peak at -5 ppm corresponds to a  $\text{SiN}_2\text{C}_2$  surrounding within a six-membered cyclosilazane-ring.<sup>6</sup> For example, a  $\text{SiN}_2\text{C}_2$  group in a four- or eight-membered ring would cause a chemical shift of 3.3 ppm or -8.7 ppm respectively.<sup>6</sup> A  $\text{SiN}_2\text{C}_2$  group in a chain would have a chemical shift of 2.2 ppm.<sup>5</sup> Such signals are not found in the spectrum. Thus, it is definitely proved that the molecule consists of six-membered rings. As these results show, the polymer has a structure of con-

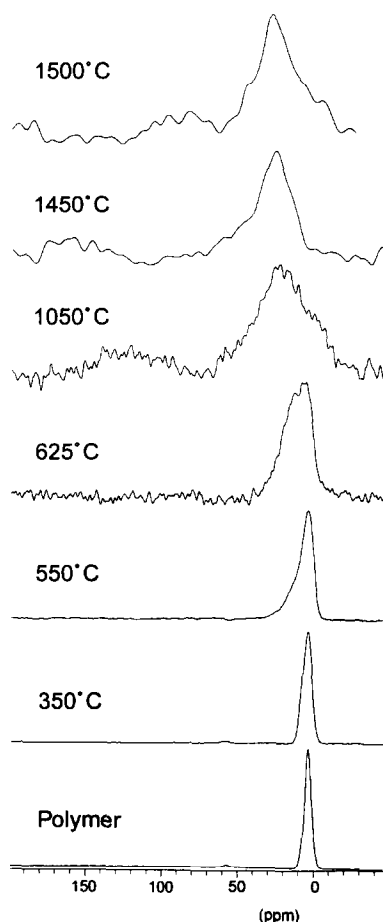


Fig. 1.  $^{13}\text{C}$ -NMR-MAS-spectra of NCP 200 and temperature treated derivatives.

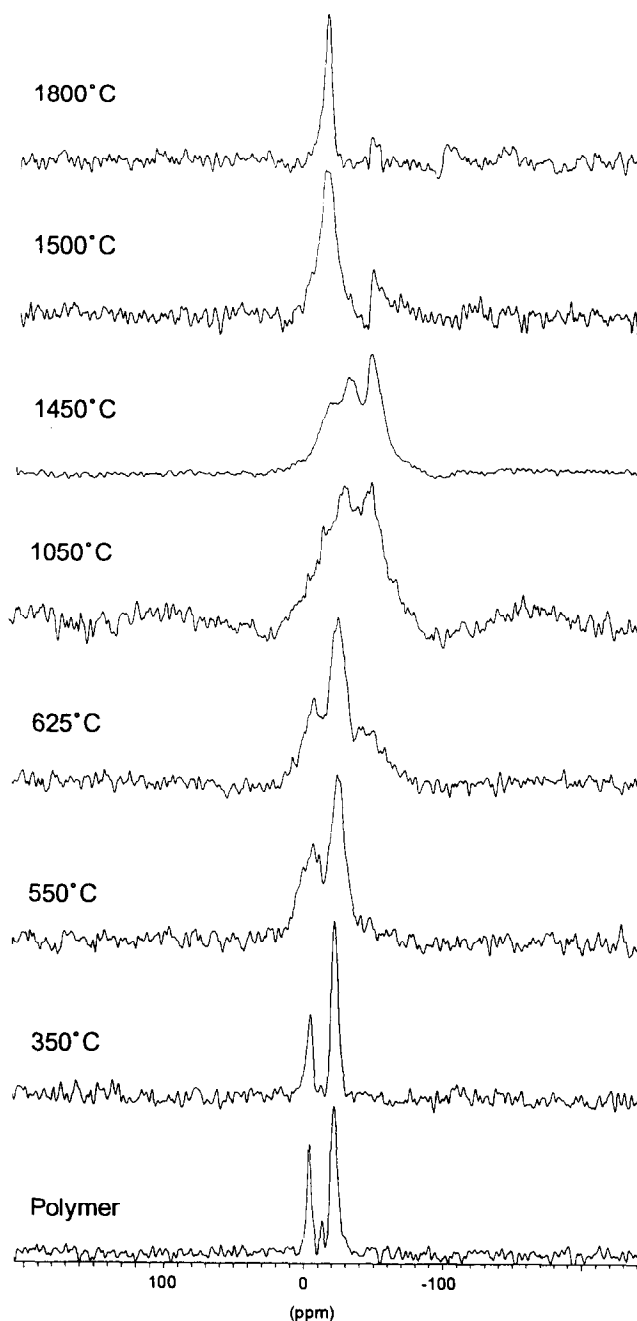


Fig. 2.  $^{29}\text{Si}$ -NMR-MAS-spectra of NCP 200 and temperature treated derivatives.

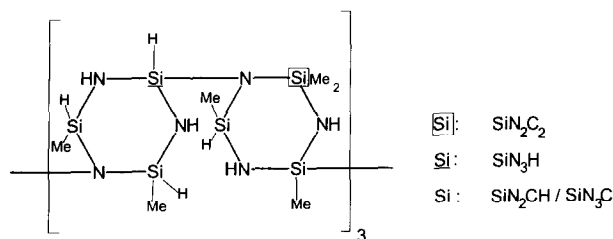
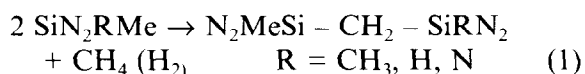


Fig. 3. Chemical structure of the polymer (NCP 200).

nected six-membered rings. The bridging Si-atoms could have a  $\text{SiN}_3\text{H}$  or  $\text{SiN}_3\text{C}$  environment. The peak at  $-14$  ppm is assigned to the bridging  $\text{SiN}_3\text{H}$  sites in the six-membered ring. As the signal is weak, the bridging  $\text{SiN}_3\text{H}$  sites have a low abundance. The bridging Si-atoms with  $\text{SiN}_3\text{C}$  environment have a chemical shift of  $-23.8$  ppm. The small amount of these  $\text{SiN}_3\text{C}$  groups is superimposed by the  $\text{SiN}_2\text{CH}$  peak at  $-22$  ppm. The relation between  $\text{SiN}_2\text{C}_2$  and  $\text{SiN}_2\text{CH}$  sites is determined as 1:2 by calculating the appropriate signal areas. The structure proposal of the NCP 200 polymer in Fig. 3 is based on these results. The producer gives a value of 1100 g/mol for the molecular weight average. Thus one average molecule consists of about six six-membered rings.

### 3.1.2 350°C product

After heat treatment of the polymer at 350°C all the signals in the spectra slightly broaden. The chemical shift of the signal in the  $^{13}\text{C}$ -spectra slightly increases. This is caused by the formation of  $\text{CH}_2$ -bridges shown in the following crosslinking reaction:



$\text{CH}_2\text{Si}_2$  sites cause a chemical shift of 12 ppm.<sup>7</sup> The  $^{13}\text{C}$ -signal has slightly shifted towards the high-field side. This indicates that the crosslinking reaction mentioned above takes place in small amounts.

In the  $^{29}\text{Si}$ -spectra, the described reaction causes a slight increase of the line widths. The chemical environment of the appropriate atoms is slightly modified by the crosslinking reaction, which is shown by the broadening of the signals. The chemical shifts and the relation of the peak areas remain essentially unchanged. The structure is shown in Fig. 4.

### 3.1.3 550°C product

At this temperature, in the  $^{13}\text{C}$ -spectra an additional signal at 12 ppm is found as a shoulder, which is attributed to  $\text{CH}_2$ -bridges. The crosslinking reaction mentioned above intensifies and hence the number of  $\text{CH}_2$ -bridges increases.

This reaction can occur with all kinds of Si-species. The  $^{29}\text{Si}$ -spectrum shows further broadening

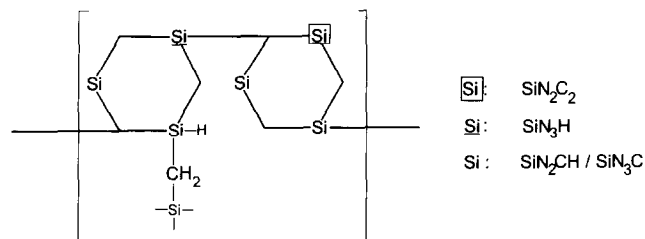


Fig. 4. Chemical structure of the 350°C product (NCP 200).

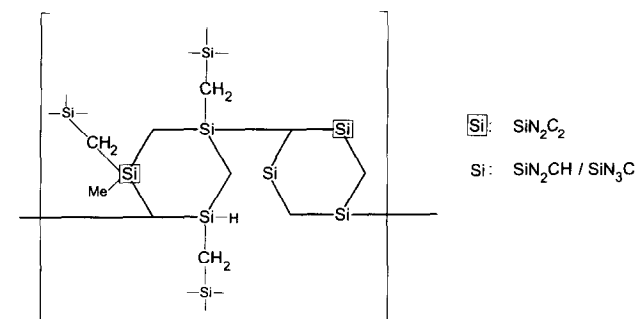
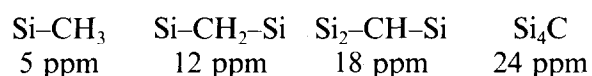


Fig. 5. Chemical structure of the 550°C product (NCP 200).

of the lines. Thus the signals of the  $\text{SiN}_2\text{CH}$  and  $\text{SiN}_3\text{H}$  sites combine. The comparison of one-pulse and CP-spectra shows a strong reduction in intensity for the H-amount in the molecule. The Si-H-bonds react more easily than the Si-C-bonds with Si- $\text{CH}_3$  to form a  $\text{CH}_2$ -bridge (see eqns (5) and (6)). Thus the number of  $\text{SiN}_2\text{C}_2$  sites increases at the expense of the  $\text{SiN}_2\text{CH}$  sites. The ratio of  $\text{SiN}_2\text{C}_2$  and  $\text{SiN}_2\text{CH}$  is now determined as 1:1 (ratio of the appropriate peak areas). In addition, the Si-H-bonds of the bridging Si-atoms react to form  $\text{CH}_2$ -bridges. Thus the small amount of  $\text{SiN}_3\text{C}$  sites with the chemical shift of  $-23.8$  ppm included in the  $\text{SiN}_2\text{CH}$ -signal at  $-22$  ppm slightly increases. The structure is shown in Fig. 5.

### 3.1.4 625°C product

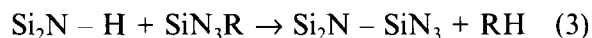
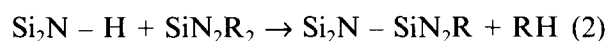
At this temperature, the successive increase of the chemical shift in the  $^{13}\text{C}$ -spectrum continues. This is caused by the increased coordination of the C-atoms with Si-atoms.<sup>8</sup> If the known  $\delta$ -values for Si- $\text{CH}_3$  (5 ppm),<sup>4</sup> for  $\text{Si}_2\text{CH}_2$  (12 ppm)<sup>7</sup> and for  $\text{Si}_4\text{C}$  (24 ppm)<sup>4</sup> are interpolated, it is found a  $\delta$ -value of 18 ppm for the  $\text{Si}_3\text{CH}$  site:



Therefore the signal at 15 ppm in the  $^{13}\text{C}$ -spectra is assigned to a coordination of the C-atoms with more than two Si-atoms. The  $\text{Si}_2\text{CH}_2$ -bridges formed in the reactions described above can react with methyl or hydrogen to form  $\text{Si}_3\text{CH}$  groups, resulting in the formation of a dense network.

The  $^{29}\text{Si}$ -spectrum shows a signal at 43 ppm for the first time which is assigned to  $\text{SiN}_4$  sites.<sup>5,9</sup>

These are formed by the following crosslinking reactions of the NH-groups:



Consequently, the number of  $\text{SiN}_4$  sites determined from the peak area is enhanced by up to 30%. In addition, the amount of  $\text{SiN}_3\text{C}$  sites (−24 ppm) increases at the expense of the  $\text{SiN}_2\text{C}_2$  sites (−7 ppm). Since the  $\text{SiN}_2\text{CH}$  sites and the  $\text{SiN}_3\text{C}$  sites have a combined signal and the amount of  $\text{SiN}_2\text{CH}$  decreases (reaction of the Si–H-bond with NH or  $\text{CH}_3$ ), the intensity of the signal remains constant. The structure is shown in Fig. 6.

### 3.1.5 1050°C product, amorphous ceramic

In the  $^{13}\text{C}$ -spectrum, the chemical shift of the signal is increased still. It now is found at 24 ppm, which is attributed to  $\text{Si}_4\text{C}$ .<sup>4</sup> The comparison of one-pulse and CP-spectra shows only a small amount of H-atoms remaining in the molecule. The last H-atom of the  $\text{Si}_3\text{CH}$ -group reacts, forming the  $\text{SiC}_4$ -group.

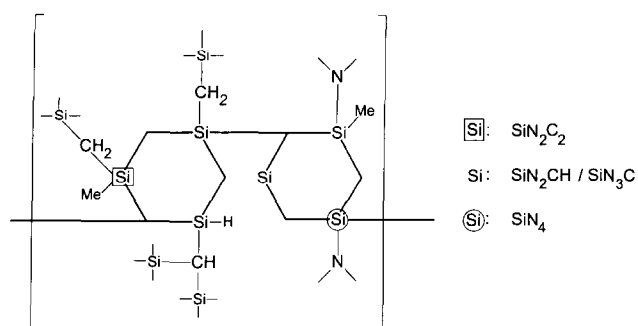


Fig. 6. Chemical structure of the 625°C product.

That is the reason for the reduction of the H-atoms.

Figure 7 shows the  $^{29}\text{Si}$ -spectrum fitted with three signals to estimate the intensities of the appropriate components. In general it remains unchanged from the 625°C product. Only the line broadening has continued. The structure (Fig. 8) shows that the basic structure  $\text{SiN}_4$ , necessary to form the thermodynamically stable phase silicon nitride, has already preformed in the amorphous state.

At the C-atoms all H-atoms are now replaced by Si-atoms. Thus the presupposition to form silicon carbide is made. In the amorphous state, the  $\text{SiN}_4$  sites as well as the  $\text{CSi}_4$  sites are still fixed in the network.

At lower temperatures, the  $^1\text{H}$ -spectra show a methyl-signal becoming continuously weaker as the temperature is increased and the number of H-atoms is decreased. At 1050°C, it is no longer possible to detect this signal. This indicates the reduction of the H-atoms.

### 3.1.6 1500°C product, crystalline ceramic

In the  $^{13}\text{C}$ -spectrum the SiC- signal is found at 27 ppm (corresponding to the measured SiC-sample).

The  $^{29}\text{Si}$ -spectrum shows the  $\text{Si}_3\text{N}_4$ - signal at −47 ppm and the SiC- signal at −18 ppm (corresponding to the measured  $\text{Si}_3\text{N}_4$ - and SiC-standards). At this temperature the preformed  $\text{Si}_4\text{C}$  and  $\text{SiN}_4$  sites have formed the thermodynamically stable crystalline phases silicon carbide and silicon nitride.<sup>3</sup> The ceramic has changed from the amorphous state into the multiphase state. At the same time a decomposition reaction occurs. Excess carbon reacts with silicon nitride.<sup>10</sup>

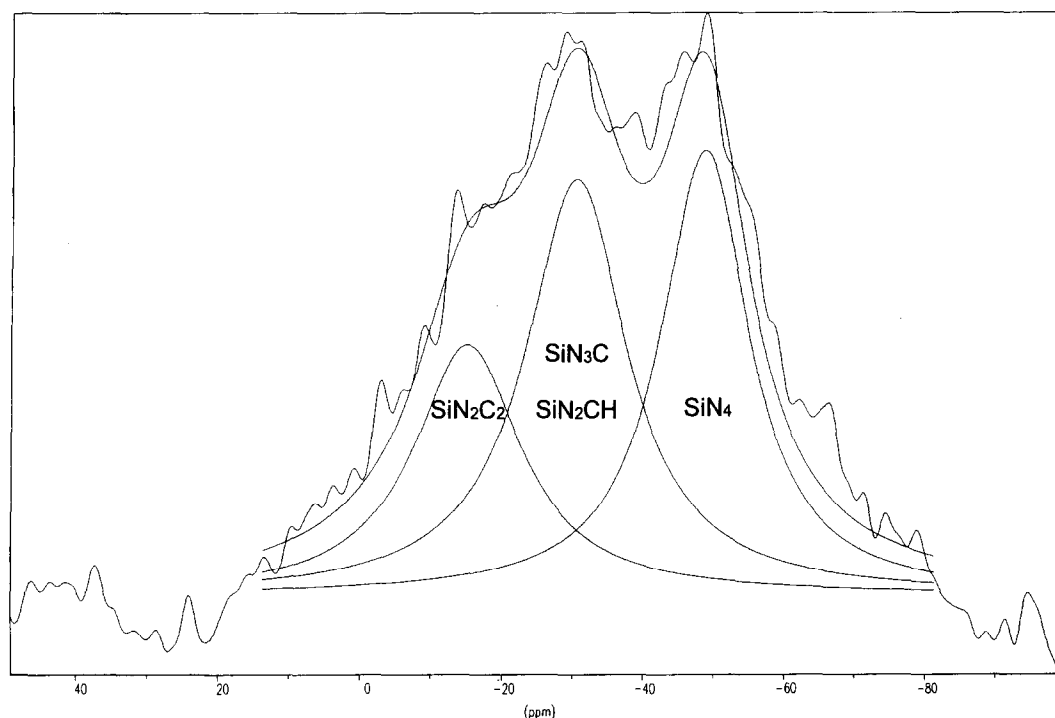


Fig. 7.  $^{29}\text{Si}$ -spectrum of the amorphous ceramic fitted with three signals.

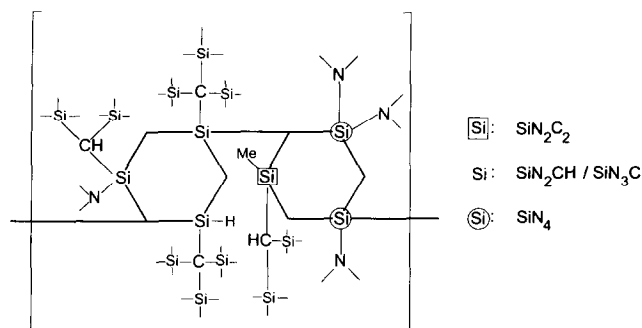


Fig. 8. Chemical structure of the amorphous ceramic.

Table 1. Dissociation energies  $\Delta E$  (kJ/mol) for 298 K<sup>13</sup>

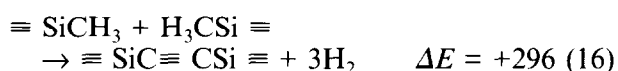
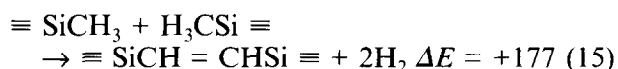
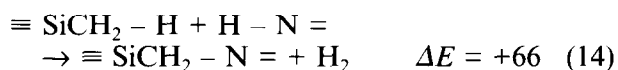
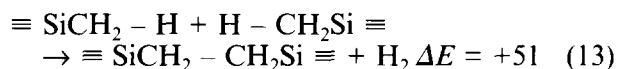
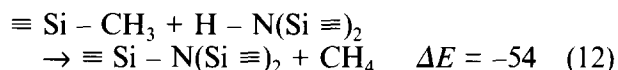
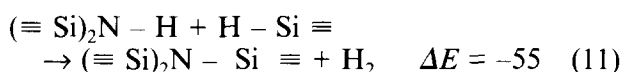
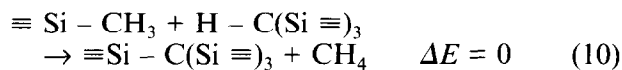
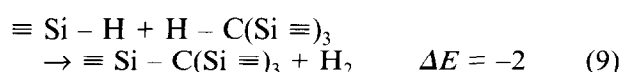
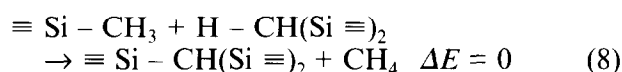
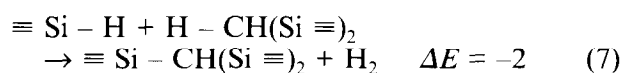
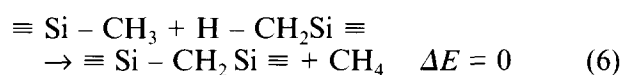
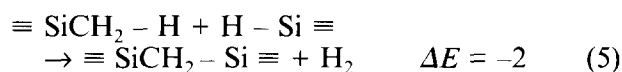
Element	H	C	N	Si
H	436	416	391	323
C	416	345	305	306
N	391	305	159	335
Si	323	306	335	202

The dissociation energy for a C=C-double bond is 615 kJ/mol and for a C  $\equiv$  C-triple bond 811 kJ/mol.

As the crystallization temperature increases, the detection of the crystalline phases becomes more difficult.<sup>9</sup> To get an acceptably good signal to noise ratio the repetition time had to be increased up to 10 min for the 1800°C product.

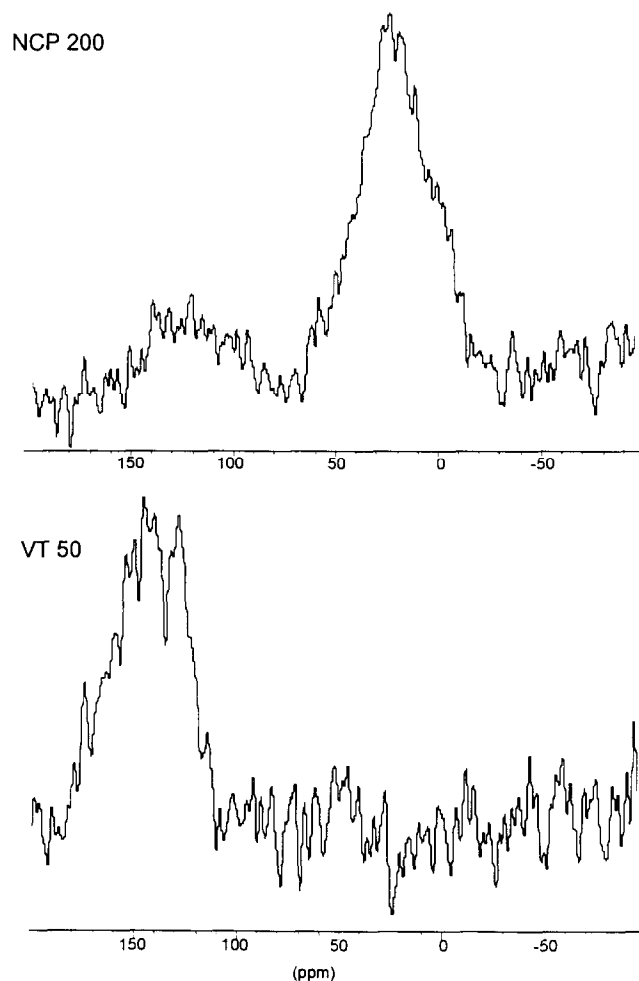
The reactions and structures described above are also confirmed by infrared spectroscopy<sup>11</sup> and energetic calculations. The amounts of energy for the assumed reactions are calculated using the appropriate dissociation energies.<sup>11</sup> Table 1 lists the values for homolytic dissociation.

The following equations show the assumed reactions with the appropriate calculated reaction enthalpy  $\Delta E$  (kJ/mol).



The reactions (5)–(10) describe the successive conversions around the C-atom. With a  $\Delta E$ -value around 0 they should take place easily at higher temperatures. The NMR investigations that show these reactions to occur at temperatures above 300°C give evidence for this consideration.

A difference was found between the energetic calculations and the NMR results for only reactions (11) and (12). The described reactions of the N–H-bond should occur easily at lower temperatures. However, as the NMR experiments show, they are found only above 600°C. This may be caused by a kinetic effect.

Fig. 9. <sup>13</sup>C-spectra of the amorphous ceramics of NCP 200 and VT 50 in comparison.

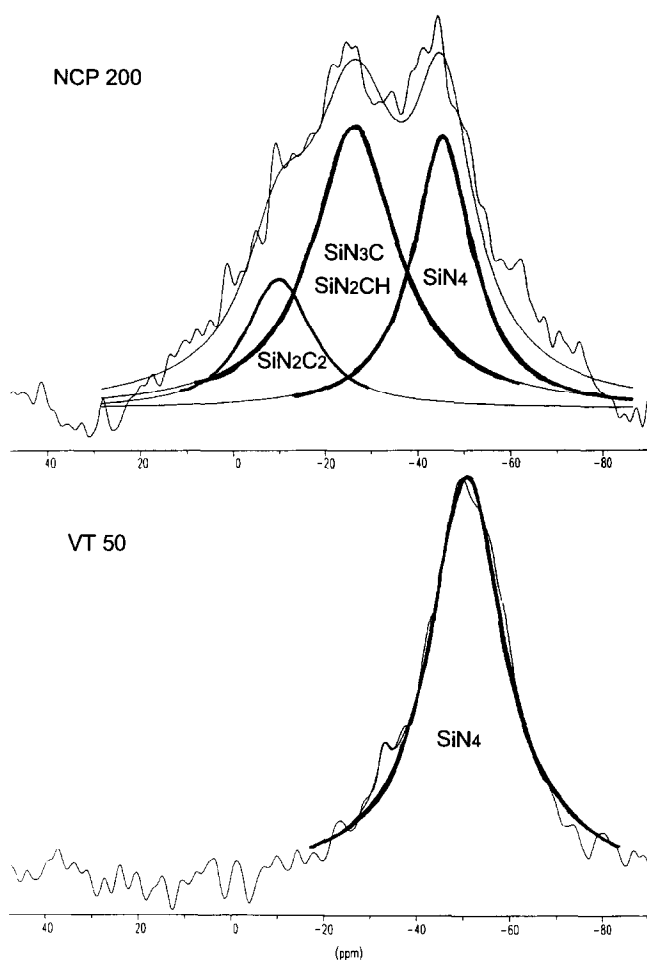


Fig. 10.  $^{29}\text{Si}$ -spectra of the amorphous ceramics of NCP 200 and VT 50 in comparison.

The last four reactions (13)–(16) are energetically unfavourable and do not take place, which is in accordance with the results of the NMR investigations.

### 3.2 VT 50

The  $^{13}\text{C}$ -spectra show a significant difference between the two amorphous materials NCP 200 and VT 50. In contrast to NCP 200, a signal centered around 140 ppm is detected in the case of VT 50, indicating a high amount of  $sp^2$ -carbon<sup>8</sup>

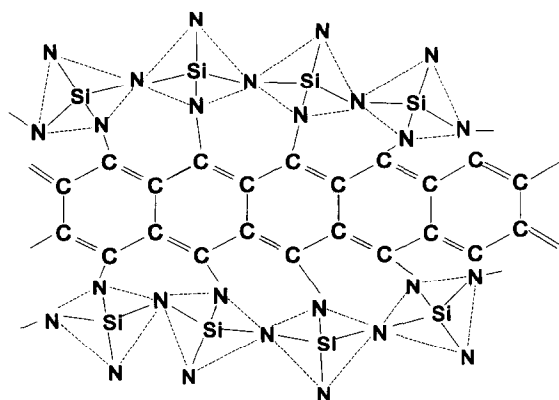


Fig. 11. Structure proposal of the amorphous state obtained by pyrolysis of the polysilazane VT 50 at 1050°C.

(Fig. 9). The vinylic groups of the VT 50 polymer are the reason for the appearance of  $sp^2$ -carbon in the amorphous ceramic, resulting in an increased electric conductivity of the amorphous VT 50 in comparison to the amorphous NCP 200 which will be published separately.

The  $^{29}\text{Si}$ -spectrum of the amorphous NCP 200 exhibits the signals of the different Si sites described in section 3.1. In contrast to this result, the spectrum of the amorphous VT 50 shows only one single peak that represents  $\text{SiN}_4$  sites (Fig. 10). This difference is caused by the different polymer structure of the VT 50. In the polymer, every Si-atom is surrounded by three N-atoms. Thus in the crosslinking reactions the  $\text{SiN}_4$  sites are directly formed and in the amorphous ceramic nearly all Si-atoms are surrounded by four N-atoms. Another possibility of explaining is the presence of C–N bonds in the end groups of the VT 50 polymer. According to Laine *et al.*<sup>12</sup> C–N bonds support the formation of  $\text{SiN}_4$  sites. Figure 11 shows a structure proposal of the amorphous VT 50.

## 4 Conclusion

The molecular mechanisms occurring during the transformation of the polysilazane NCP 200 into amorphous and crystalline ceramics in the temperature range between room temperature and 1800°C were determined by solid state NMR spectroscopy. It was possible to suggest structural formulas for the appropriate intermediates. The obtained results confirm with energetic calculations. It was found that NCP 200 crystallizes between 1450 and 1500°C.

The comparison of the NCP 200 with a polyvinylsilazane (VT 50) shows significant differences in the  $^{13}\text{C}$ - and  $^{29}\text{Si}$ -spectra of the amorphous materials. Pyrolysis of the polymer VT 50 yields a ceramic residue which contains a high amount of  $sp^2$ -carbon and  $\text{SiN}_4$  sites whereas the NCP 200-derived amorphous state contains various different Si-sites.

## References

1. Rice, R., *Ceram. Bull.*, **62** (1983) 889.
2. Seyferth, D. & Wiseman G. H., *J. Am. Ceram. Soc.*, **67** (1984) 132.
3. Frieß, M., Bill, J., Aldinger, F., Szabo, D. V. & Riedel R., *Key Engineering Materials*, **89–91** (1994) 95.
4. Mocaer, D., Pailler, R., Naslain, R., Richard, C., Pillot J. P., Dunogues, J., Gerardin, C. & Taulelle, F., *J. Mater. Sci.*, **28** (1993) 2615.
5. Gerardin, C., Taulelle, F. & Livage, J., *Mat. Res. Soc. Symp. Proc.*, **287** (1993) 233.

6. Yive, N. S. C. K., Corriu, R., Leclercq, D., Mutin, P. H. & Vioux, A., *New J. Chem.*, **15** (1991) 85.
7. Schmidt, W. R., Interrante, L. V., Doremus, R. H., Trout, T. K., Marchetti, P. S. & Maciel, G. E., *Chem. Mater.*, **3** (1991) 257.
8. Soraru, G. D., Babonneau, F. & Mackenzie, J. D., *J. Mater. Sci.*, **25** (1990) 3886.
9. Carduner, K. R., Carter, R. O., Millberg, M. E. & Crosbie, G. M., *Anal. Chem.*, **59** (1987) 2794.
10. Weiss, J., Lukas, H. L., Lorenz, J., Petzow, G. & Krieg, H., *Calphad*, **5** (1981) 125.
11. Frieß, M., PhD thesis, University of Stuttgart (1994).
12. Laine, R. M., Babonneau, F., Rahn, J. A., Zhang, Z.-F. & Youngdahl, K. A., *37th Sagamore Army Materials Conference*.
13. Hollemann, A. F. & Wiberg E., *Lehrbuch der Anorganischen Chemie*, de Gruyter, Berlin-New York, 91–100 Aufl, 1985, p. 139.